SEMARAK ILMU PUBLISHING

CFD Letters

Journal homepage:
https://semarakilmu.com.my/journals/index.php/CFD_Letters/index
ISSN: 2180-1363

Application of Box- Behnken Design with Response Surface Methodology to Analyse Friction Characteristics for Corrugated Pipe via CFD

Azraf Azman[1,2], Mohd Zamri Yusoff[1,*], Azfarizal Mukhtar[1], Prem Gunnasegaran[1], Ng Khai Ching[3], Ahmad Shah Hizam Md Yasir[4]

[1] College of Engineering, Putrajaya Campus, Universiti Tenaga Nasional (UNITEN), Jalan IKRAM-UNITEN 43000 Kajang Selangor, Malaysia
[2] Agensi Nuklear Malaysia, Bangi, 43000 Kajang, Selangor, Malaysia
[3] University of Nottingham Malaysia Campus, Jalan Broga, 43500 Semenyih, Selangor, Malaysia
[4] Rabdan Academy, 65, Al Inshirah, Al Sa'adah, Abu Dhabi, 22401, UAE

ARTICLE INFO

Article history:
Received 6 September 2022
Received in revised form 8 October 2022
Accepted 7 November 2022
Available online 1 July 2023

Keywords:
Hybrid Nanofluids; Corrugated Tube; CFD; Response Surface Method; Friction Factor

ABSTRACT

Due to the fact that modern technologies are getting smaller and more compact and are anticipated to perform better, there has been an increase in interest in heat transfer enhancement employing hybrid nanofluids in tubes and channels in recent years. This study seeks to establish an outward saw tooth corrugated wall model-based predictive friction characteristic for internal tube flow. Computational Fluid Dynamics (CFD) was used to simulate the model numerically. The response behaviour study was then conducted utilising the Design of Experiment (DOE) and the Response Surface Methodology (RSM). The established surrogate model has led to the consideration of RSM. In this study, the DOE was executed by utilising the Box-Behnken Design (BBD) method with two-level factorial by considering three parametric factors which are: (a) 10000 to 30000 axial Reynolds number, Re, (b) 1mm to 4mm wave amplitude, a, and (c) 5mm to 20mm wavelength, lw. The results showed that the expected response surface values are consistent with the CFD values and that the predictive model is therefore reliable. The R-squared (R^2) value is 98.25%, indicating that the model can predict new observations. The wavelength and wave amplitude show significant factors influencing the friction factor which is -0.11235 and 0.14861 respectively and this is based on the normal plot of the effect from the regression model from RSM. These results provide data for estimating the geometric characteristics of tube corrugated wall.

1. Introduction

Various techniques have been developed over the past few decades to improve the heat transfer rate or efficiency of traditional heat transfer devices in a variety of engineering applications, such as radiators in automobiles [1], micro channel in micromachining technology [2], cooling electronic components, and refrigeration systems. These strategies proposed by early scientists fall into two groups: active technique and passive technique [3]. Active procedures often necessitate the use of

* *Corresponding author.*
E-mail address: zamri@uniten.edu.my (Mohd Zamri Yusoff)

https://doi.org/10.37934/cfdl.15.7.113

an external power source and may involve mechanical components, whereas passive approaches are independent of external sources. As a result, passive approaches have been actively investigated because they can reduce existing system operating costs while maintaining excellent reliability [3].

Numerous passive approaches were utilised, including the incorporation of fins, well-engineered surface texturing [4] and micro channels. In addition, the application of innovative coolants with improved thermophysical properties has attracted attention as they appear to be an alternative for conventional heat transfer fluids with low thermal conductivity, such as water, oil, ethylene glycol, etc [1]. There was evidence that scientists were attempting to include high thermal conductivity millimetre and micrometre scaled particles in conventional coolants to create a blend with increased thermal characteristics. In addition to causing a high-pressure drop, obstructing the flow, and even corroding the heat exchanger system's components, this strategy was deemed less convincing.

Choi *et al*., [5] report that the development of powder manufacturing techniques has led to the synthesis of nanosized particles. The nanofluids are colloidal suspensions created by dispersing solid nanoparticles (10 to 100 nm) in a base fluid to improve their transport properties. The addition of solid nanoparticles can also enhance the thermal properties of base fluids [6-8]. These materials have unique optical, electrical, and chemical properties. Nanofluid is a novel heat transfer fluid created by dispersing nanometer-sized solid particles in conventional heat transfer fluids such as water or ethylene glycol to improve thermal conductivity and, consequently, heat transfer performance. It is known that the effectiveness of heat transfer enhancement is dependent on variables such as the number of dispersed particles, material type, particle shape, particle volume fraction, and so on.

The primary goal of synthesising hybrid nanofluids is to obtain the properties of their constituent materials. It is not possible for a single material to possess all the desirable properties required for a specific application; it may have either good thermal properties or good rheological properties. In many practical applications, however, it is necessary to compromise between multiple properties, and this is where hybrid nanofluids come into play. Due to the synergistic effect, the hybrid nanofluid is anticipated to have a higher thermal conductivity than individual nanofluid [9-12]. Chein and Chuang [13] found in their investigation that a CuO-H_2O nanofluid suspension may absorb more heat and result in a lower wall temperature than pure liquid. The penalty was a small pressure drop increase. Nonetheless, a study demonstrates that by distributing composite nanoparticles in the base fluid (hybrid nanofluid), heat transfer performance is improved compared to nanofluid containing single nanoparticles [12].

Response Surface Methodology (RSM), however, has been used to increase the design's effectiveness. The objective of RSM is to discover and study the quantitative assessment of numerous design parameters that affect the thermal performance of the corrugated tube [6,8,14,15]. This study seeks to develop a statistical data-based metamodel method that can be used to examine the association between input variables (factors) and output variables (response) in order to discover the friction factor utilising the RSM. Similarly, a numerical study on "saw tooth" corrugated wall geometry turbulent-forced convective heat transfer of Al2O3-CuO/water (Alumina/Copper Oxide-water hybrid nanofluid with the concentration of 0.05% of 80% of Al2O3 to 20% of CuO (80:20) ratio using CFD and as most flows in engineering applications such as corrugated pipe are turbulent flow.

2. Methodology

2.1 Physical Model and Assumptions

The two-dimensional corrugated circular pipes used in the simulations are cylindrical pipes with periodically distributed diametrically symmetric roughness on the wall. According to Kaood *et al.,* [16] inward or outward corrugated shapes have higher performance evaluation criterion compared

to smooth tubes. A generic, schematic representation of the corrugated pipe is shown in Figure. 1. The heat transfer was performed numerically using a corrugated pipe with an inner diameter of 10 mm. The total lengths of the hydrodynamic development section and the test section provide a maximum length-to-diameter ratio (LT/d) of 80. The length-to-diameter ratio of the investigated region is L1/d=20, and the length-to-diameter ratio of an upstream section is L/d=40 to ensure a fully developed flow in the test section ((L/d)>10). The length-to-diameter ratio of the downstream section (exit section) is L2/d=20 which is used to prevent any reversed flow through the computational domain. The roughness parameters are determined by the rib height (a), and wavelength (Lw). In this work the triangular roughness parameters are expressed in the form of dimensionless roughness parameters: the rib pitch-to-tube diameter ratio (Lw/d) was in the range of 0.5–2.0 and the rib height-to-tube diameter ratio (a/d) was in the range of 0.1–0.4, The following assumptions are adopted in this work: (i) the ribs and the grooves are periodically distributed in the axial direction; (ii) the flow is steady, fully developed, turbulent, and two-dimensional; (iii) the tube material is homogeneous and isotropic; and (iv) the thermal conductivity of the tube wall material does not change with temperature.

2.2 Governing Equations

The geometry under study is two-dimensional in a rectangular plane. The flow is steady, incompressible, forced turbulent convection through the straight corrugated circular pipe and assumed to be axisymmetric along the horizontal plane parallel to the x-axis. The flow and thermal fields are described by the two-dimensional, steady continuity, momentum, energy equations and constant thermophysical properties [10,11].

The continuity equation is:

$$\frac{\partial}{\partial x_i}(\rho u_i) = 0 \tag{1}$$

where, ρ is the density of fluid and u_i is the axial velocity.

Conservation of momentum

$$\frac{\partial}{\partial x_i}\left(\rho u_i u_j\right) = -\frac{\partial P}{\partial x_i} + \frac{\partial}{\partial x_j}\left[\mu\left(\frac{\partial u_i}{\partial x_j} + \frac{\partial u_j}{\partial x_j}\right) - \frac{2}{3}\mu\frac{\partial u_i}{\partial x_i}\delta_{ij} - \overline{\rho u'_\iota u'_j}\right] \tag{2}$$

Conservation of energy

$$\frac{\partial}{\partial x_i}\left(\rho u_j C_p T\right) = -\frac{\partial}{\partial x_i}\left(\lambda\frac{\partial T}{\partial x_j} + \frac{\mu_t}{\sigma_{h,t}}\frac{\partial\left(C_p T\right)}{\partial x_j}\right) + u_j\frac{\partial P}{\partial x_j} + \left[\mu\left(\frac{\partial u_i}{\partial x_j} + \frac{\partial u_j}{\partial x_j}\right) - \frac{2}{3}\mu\frac{\partial u_i}{\partial x_i}\delta_{ij} - \overline{\rho u'_\iota u'_j}\right]\frac{\partial u_i}{\partial x_j} \tag{3}$$

where $-\overline{\rho u'_\iota u'_j}$ are the Reynolds stress, u_i and u_j are the time-averaged velocity for i and j directions. Time-averaged temperature, fluid thermal conductivity, density, turbulent Prandtl number for energy, turbulent viscosity and time-averaged pressure are stated as T, λ, ρ, $\sigma_{h,t}$, μ_t and P, respectively.

In the numerical study, the realizable k–ε turbulence model is used in order to give fast and accurate results [10-12,17,18]. Therefore, turbulent dissipation rates (ε) and transport of turbulence kinetic energy (k) equations should be considered.

k equation

$$\frac{\partial}{\partial x_j}(\rho k u_j) = \frac{\partial}{\partial x_i}\left[\left(\mu + \frac{\mu_t}{\sigma_k}\right)\frac{\partial k}{\partial x_j}\right] + G_k - \rho\varepsilon \tag{4}$$

ε equation

$$\frac{\partial}{\partial x_j}(\rho \varepsilon u_j) = \frac{\partial}{\partial x_i}\left[\left(\mu + \frac{\mu_t}{\sigma_\varepsilon}\right)\frac{\partial \varepsilon}{\partial x_j}\right] + \rho C_1 S\varepsilon - \rho C_2 \frac{\varepsilon^2}{k+\sqrt{\upsilon\varepsilon}} \tag{5}$$

Turbulent Prandtl number is expressed as σ_k and σ_ε regarding *k* and *ε* in Eq. (14) and Eq. (15). Eq. (16) represents the turbulent viscosity.

$$\mu_t = \rho C_\mu \frac{k^2}{\varepsilon} \tag{6}$$

with C_1*= 1.44,* C_2 = 1.9, σ_k = 1, σ_ε = 1.2

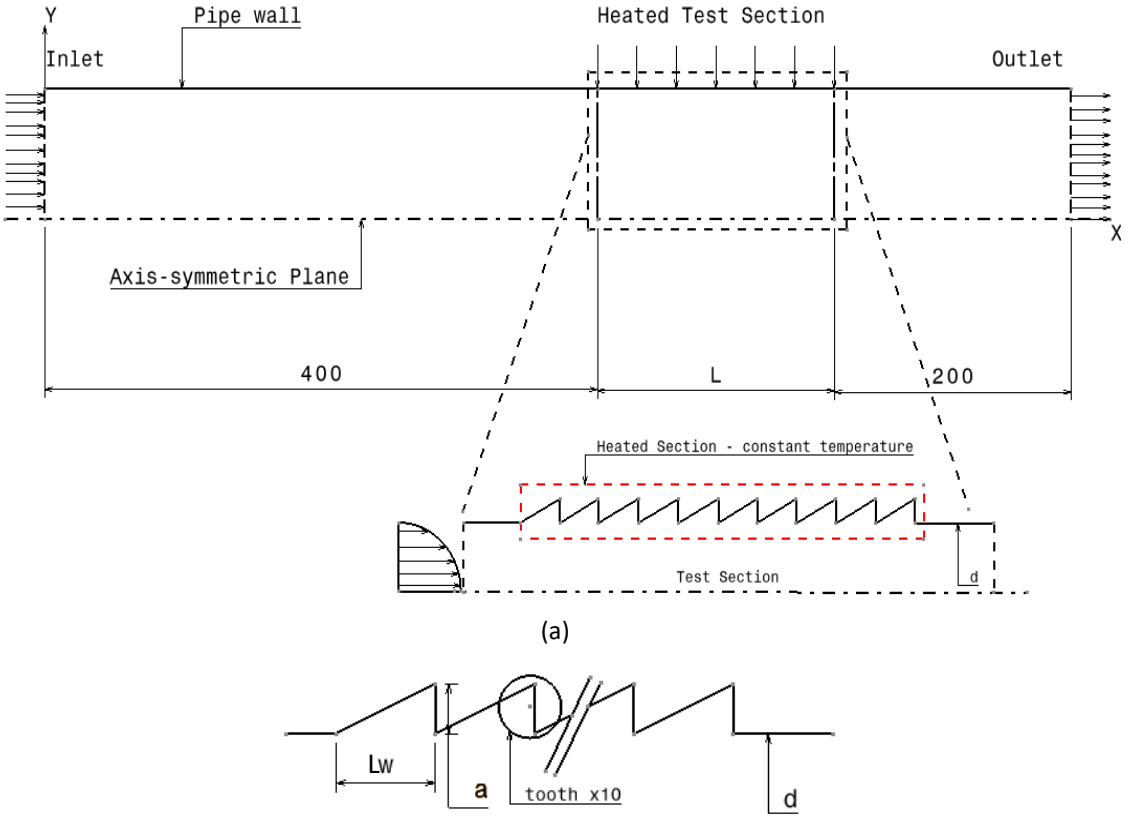

Fig. 1. Schematic diagram of physical model, showing the test section and the boundary conditions

2.3 Thermophysical Properties of Hybrid Nanofluid

These equations are general and can be applied in mono and hybrid nanoparticles with the suitable modifications, the base fluid is symbolized with (bf), the nanoparticle with (np) and the nanofluid with (nf), while the volume concentration of the total nanoparticle in the fluid with (Ø). It

is important to state that in this study, the nanoparticle "Al_2O_3" is symbolized with the number "1" and the nanoparticle "CuO" with the number "2". Bellos and Tzivanidis [19] calculate the total concentration for the hybrid nanofluid (∅) using the following:

$$\emptyset = \emptyset_1 + \emptyset_2 \tag{7}$$

These following equations give the density, the specific heat capacity and the thermal conductivity of the equivalent nanoparticle of concentration (∅) and aids to the further calculation of the hybrid nanofluid thermal property definition according to Minea [20] and Sundar *et al.,* [21].

The density (ρ) of the equivalent nanoparticle is given as:

$$\rho_{np} = \frac{\emptyset_1 \rho_{np-1} + \emptyset_2 \rho_{np-2}}{\emptyset} \tag{8}$$

The specific heat capacity (Cp_{np}) of the equivalent nanoparticles is given as:

$$Cp_{np} = \frac{\emptyset_1 \rho_{np-1} Cp_{np-1} + \emptyset_2 \rho_{np-2} Cp_{np-2}}{\rho_{np} \emptyset} \tag{9}$$

The thermal conductivity (k_{np}) of the equivalent nanoparticles is given as:

$$k_{np} = \frac{\emptyset_1 . k_{np-1} + \emptyset_2 . k_{np-2}}{\emptyset} \tag{10}$$

The density (ρ_{nf}) of the hybrid nanofluid is given as:

$$\rho_{nf} = \rho_{bf} \,.(1 - \emptyset) + \rho_{np} \,. \emptyset \tag{11}$$

The specific thermal capacity (Cp_{nf})is given as:

$$Cp_{nf} = \frac{\rho_{bf} \,.(1-\emptyset)}{\rho_{nf}} . Cp_{bf} + \frac{\rho_{np} \,.(1-\emptyset)}{\rho_{nf}} . Cp_{np} \tag{12}$$

The thermal conductivity of the nanofluid (k_{nf}) is calculated according to the Maxwell model [22]:

$$k_{nf} = k_{bf} \frac{k_{np} + 2.k_{bf} + 2.(k_{np} - k_{bf}).\emptyset}{k_{np} + 2.k_{bf} - (k_{np} - k_{bf}).\emptyset} \tag{13}$$

The nanofluid dynamic viscosity (μ) can be calculated according to the Brinkman model [19]:

$$\mu_{nf} = \frac{\mu_{bf}}{(1-\emptyset)^{2.5}} \tag{14}$$

Table 1
Water and nanoparticles properties

Materials	ρ (kg/m^3)	Cp (J/kg.K)	k (W/m.K)	μ (Pa s)
Water	998	4182	0.597	0.000998
Alumina, Al2O3	3880	765	40	-
Copper Oxide, CuO	6350	535	69	-

3. Results

The present computations are performed for a 2-D turbulent flow of the Al2O3/CuO -water nanofluid over the corrugated saw tooth pipe. Various forms of quantitative and qualitative results can be displayed from the output of simulations, but due to the space restriction, friction factor result is presented. As presented in Table 2, hybrid nanofluids parameters are considered.

Table 2
Hybrid nanofluids properties

Nanofluids	Volume fraction, ϕ % (mixing ratio)	ρ (kg/m^3)	Cp (J/kg·K)	k (W/m·K)	μ (Pa s)	Pr
Al2O3-CuO	0.5% (80:20)	1013.885	4104.04	0.621852	0.000861	5.681

3.1 Verification and Validation

CFD results were compared with previous experimental results for validation. Grid independence studies were performed using different mesh sizes, such as 0.3mm, 0.2mm, 0.1mm, 0.09mm, and 0.08mm. Figure.2 shows the grid size for the 2D turbulent flow simulation, and Figure. 3 indicates the heat transfer Nusselt number and friction factor values obtained using different mesh sizes. Therefore, a mesh size of 0.1 mm size was selected. The 0.1 mm mesh size will be used for subsequent flow analysis. The percentage difference between 0.1mm, 0.09mm, and 0.08mm is 1-2%, which indicates that the current CFD model is reliable.

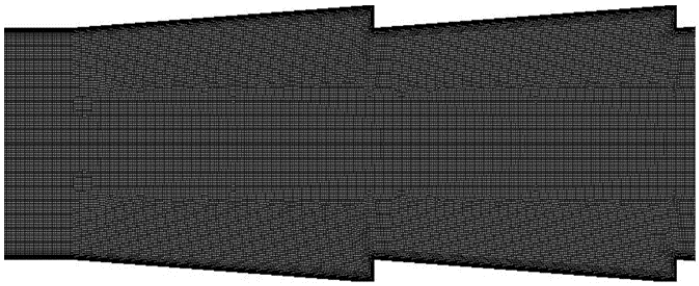

Fig. 2. Grid size of 0.1mm used for the 2D flow analysis

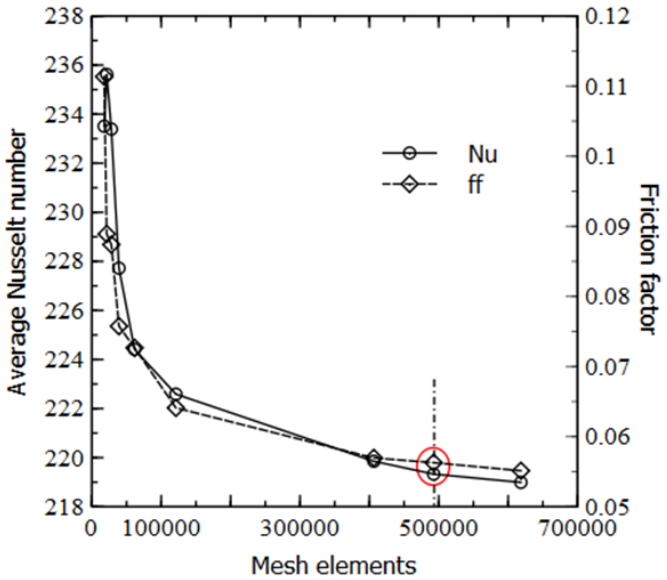

Fig. 3. Grid independence test

To assure the reliability and validity of the numerical algorithm procedure presented in the current study, the numerical results for fully developed turbulent water flow in the smooth tube were compared to the well-known empirical correlations proposed by Dittus-Boelter, Eq. (15), Petukov, Eq. (16), and Glieninski, Eq. (17) for the average Nusselt number and the correlations proposed by Filonenko, Eq. (18), McAdams, Eq. (19), and Petukhov, Eq. (20), for the friction factor.

$$Nu = 0.024Re^{0.8}Pr^{0.4} \tag{15}$$

$$Nu = \frac{RePr\left(\frac{f}{8}\right)}{1.07+12.7\left(\frac{f}{8}\right)^{0.5}\left(Pr^{\frac{2}{3}}-1\right)} \tag{16}$$

$$Nu = \frac{\left(\frac{f}{8}\right)(Re-1000)Pr}{1.0+12.7\left(\frac{f}{8}\right)^{0.5}\left(Pr^{\frac{2}{3}}-1\right)} \tag{17}$$

$$f = (1.84log_{10}Re - 1.64)^{-2} \tag{18}$$

$$f = 0.18Re^{-2} \tag{19}$$

$$f = (0.79lnRe - 1.64)^{-2} \tag{20}$$

Figure. 4 and Figure. 5 shows the comparison of the numerical Nu and ƒ with empirical correlations, respectively. Obviously, the numerical results are in good agreement with the existing correlations. It is noted that the average discrepancy of Nusselt number with Dittus-Boelter is within 11.8%, Petukov is within 4%, and Gnielinski it is within 7%, while the average discrepancy of friction factor was within 3.6%, 6.87%, and 7.9% for Filonenko, McAdams, and Petukhov correlations, respectively.

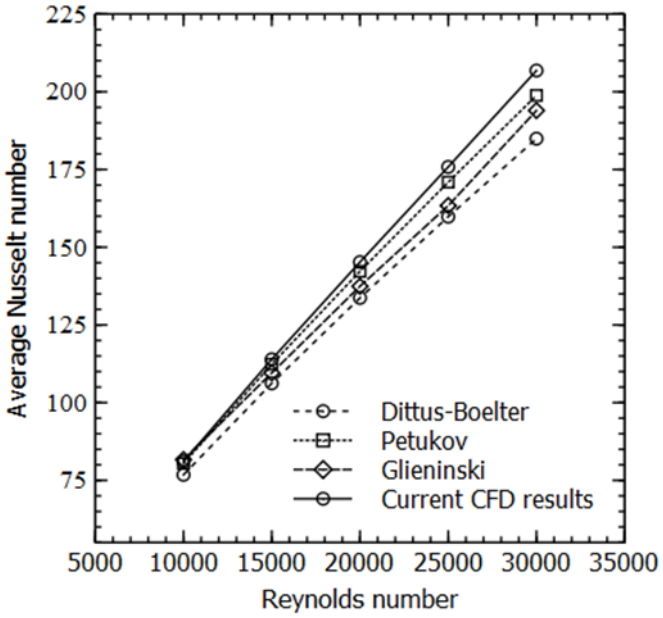

Fig. 4. Validation for smooth tube for Average Nusselt number

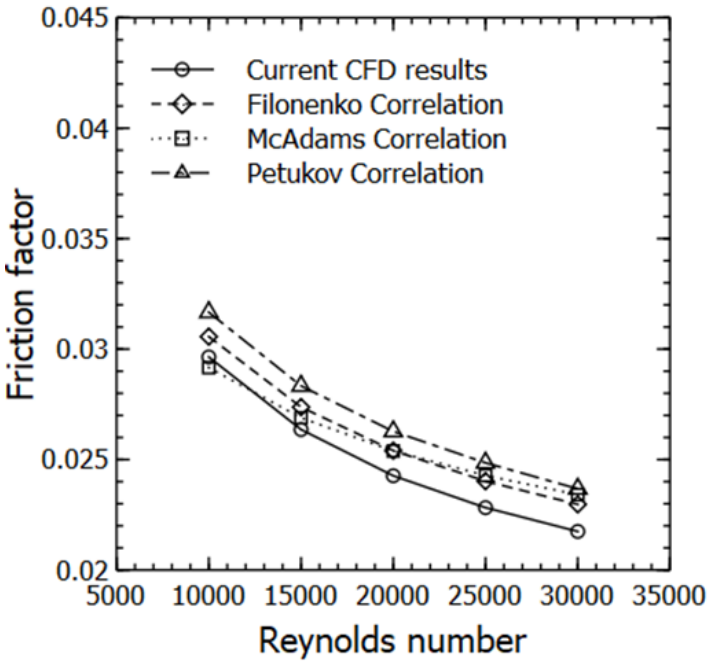

Fig. 5. Validation for smooth tube for friction factor number

As illustrated in Figure 6, the comparison shows good trend agreement between the presented numerical results and empirical correlations data. The average discrepancy of average Nusselt number with Pak-Cho is within 6.3% and Maiga *et al.,* is within 24.6%. The deviation may be related to different properties of Al_2O_3 used as an input data in the simulation.

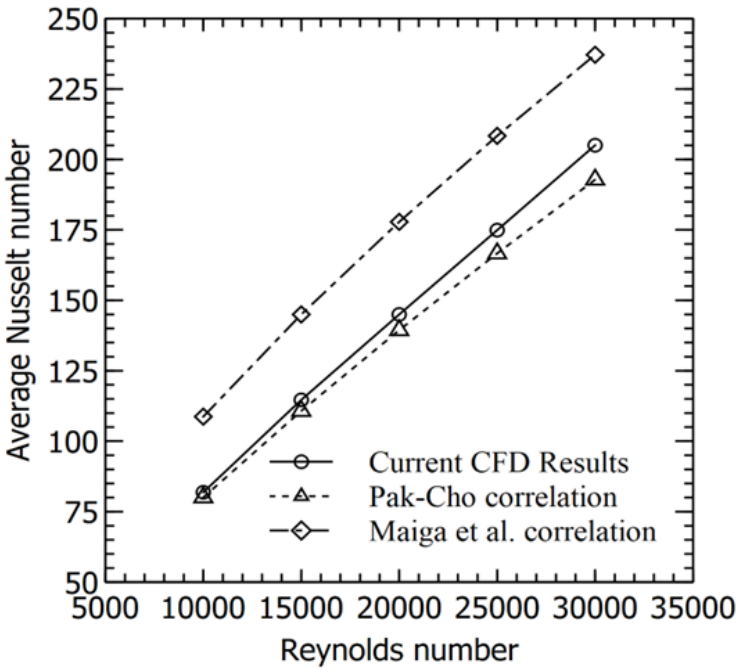

Fig. 6. Validation for smooth tube with Al_2O_3 nanofluids for Average Nusselt number

3.2 Response Surface Analysis (RSM)

RSM is known to be straightforward and computationally efficient. It can be easily constructed. RSM is a statistical modelling technique that uses regression analysis to determine $f(x)$in the observed response value ($\hat{y}$) and then estimates the effect of the independent parameters (x). A standard Design of Experiment (DOE) embedded in RSM is called Box Behnken design (BBD). BBD is an independent three-level quadratic experimental design method which does not contain an embedded factorial design. BBD method is being applied in this simulation plan. BBD is specially designed to fit a second-order model. The resulting value from RSM analysis is used to determine the polynomial equation and simplify the equation according to the influence of the factors in the final response. The three factors, which are the wavelength (Lw), amplitude (a) and Reynolds number (Re), are chosen based on Sundar *et al.,* [21] and Amani *et al.,* [22]. There are two levels of the factors listed in Table 2. The lower and Upper bounds represent the factors' low and high levels, respectively. The simulation design based on BBD for 32 factorials can be seen in Table 3.

Table 3
Factors and level of the BBD

No	Factors	Level	
		Lower bound	Upper bound
1	Lw	5	20
2	a	1	4
3	Re	10000	30000

In the current study, from three variables, 15 design points have been generated from the BBD model and then 15 CFD models must be simulated. According to the result of BBD, friction analysis based on the finite volume method (FVM) is performed to obtain the values of the different response variables. The simulation results are presented in Table 4. The response variables obtained from the simulations are then analysed by multiple quadratic regression to determine the mathematical models with the best fits. The adequacy and reliability of the regression models were also tested by using the analysis of variance (ANOVA).

Table 4
Factors and corresponding response as per CFD design used

No.	Parameters			Response	
	Lw	a	Re	CFD	RSM
1	5	4	20000	0.291983	0.298955
2	5	2.5	30000	0.276350	0.263656
3	12.5	2.5	20000	0.160232	0.160291
4	12.5	4	10000	0.207289	0.211745
5	5	1	20000	0.150803	0.167953
6	12.5	2.5	20000	0.160320	0.160291
7	5	2.5	10000	0.306728	0.295301
8	12.5	1	30000	0.079924	0.075468
9	12.5	2.5	20000	0.160320	0.160291
10	20	2.5	30000	0.151389	0.162816
11	12.5	1	10000	0.081810	0.076087
12	20	4	20000	0.188894	0.171744
13	20	1	20000	0.053222	0.046250
14	20	2.5	10000	0.134533	0.147227
15	12.5	4	30000	0.190583	0196306

After simulating the 15 design points via Ansys Fluent, the simulation friction factor was used to find the quadratic regression model. Interestingly, the predicted value obtained by the quadratic regression model agreed well with the CFD values (see Table 5). Likewise, in Figure 6, the coefficient of determination (R^2) of 98.25% is in reasonable agreement with the adjusted coefficient of determination (R^2) of 95.11%, thus indicating a well-represented response surface. The large F value is 31.27 indicates the great significance of the regression model. The associate P-values less than 0.05 for the model indicate that the model terms are statistically significant, and the effects of the model terms with a P-value greater than 0.05 are insignificant. Esfe *et al.,* [23], show R^2 and P values are 99.73% and 0.0001, respectively, in their study on optimising nanofluid flow in a double tube heat exchanger, which indicates the accuracy and great significance important of the regression model. Referring to Montgomery *et al.,* [24] and Khalid *et al.,* [25], the R^2 is called the coefficient of determination and is often used to check the adequacy of a regression model. The large value R^2 indicates that the model has successfully explained the variability in the response. From Figure 7, the predicted values obtained from the linear model agree well with the simulated values. The mathematical model for predicting the friction factor can be expressed as follows:

FF = 0.2700 - 0.03076 Lw + 0.1230 a - 0.000007 Re + 0.000785 Lw*Lw - 0.01476 a*a + 0.000000 Re*Re - 0.000122 Lw*a + 0.000000 Lw*Re - 0.000000 a*Re

Where Lw is the wavelength, a is the amplitude and Re is the Reynolds number. This equation can be used to study the response of friction factor by varying the involved parameters. For example, the positive coefficients associated with the factors a, Lw^2, Re^2, and Lw*Re reveal an increased friction factor if the factors are increased. Conversely, the negative coefficients associated with factors Lw, Re, a^2, Lw*a, and a*Re indicate decreased friction factor when these factors are increased. According to Chiang *et al.,* [26], the increase in friction factor is apparently related to pitch height and pitch-to-pitch distance and this concurs with the results of this study.

Table 5
Regression result using BBD

Source	DF	Adj SS	Adj MS	F-Value	P-Value
Model	9	0.077334	0.008593	31.27	0.001
Linear	3	0.064003	0.021334	77.63	0
Lw	1	0.030979	0.030979	112.72	0
a	1	0.032895	0.032895	119.7	0
Re	1	0.000129	0.000129	0.47	0.524
Square	3	0.012711	0.004237	15.42	0.006
Lw*Lw	1	0.007194	0.007194	26.18	0.004
a*a	1	0.004071	0.004071	14.82	0.012
Re*Re	1	0.000607	0.000607	2.21	0.197
2-Way Interaction	3	0.00062	0.000207	0.75	0.566
Lw*a	1	0.000008	0.000008	0.03	0.875
Lw*Re	1	0.000558	0.000558	2.03	0.214
a*Re	1	0.000055	0.000055	0.2	0.674
Error	5	0.001374	0.000275		
Lack-of-Fit	3	0.001374	0.000458	177441.35	0
Pure Error	2	0	0		
Total	14	0.078708			

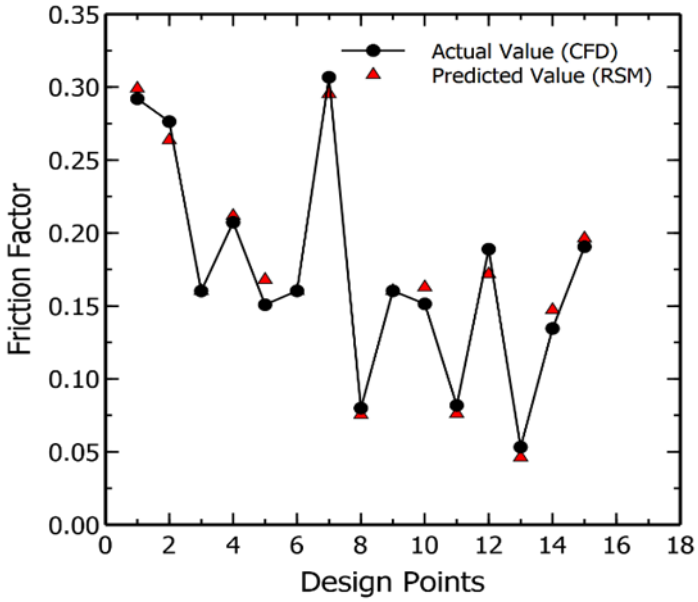

Fig. 7. Comparison of predicted value using regression model and actual value from CFD

While assessing the points on the normal probability plot in Figure 8, the plotted points fall roughly along the straight line. This observation supports the claim that the residuals are normally distributed, and the assumption of normality can be satisfied. Also, it shows that this model is appropriate for this analysis. The histogram plot follows a symmetric distribution, indicating that it is an appropriate model for the data. As shown by the versus fits plot, the residual has about the same amount of variation at all tiers of the fitted values. Therefore, it can be considered that the residuals are homoscedasticity. By performing subsequent analysis on the versus order plot, it shows no obvious and drastic pattern change. Therefore, the residual is probably mutually independent and homoscedastic with respect to run order. From the above analysis, all the assumptions required to validate the quadratic regression for this model appear to be satisfied, fit and adequate.

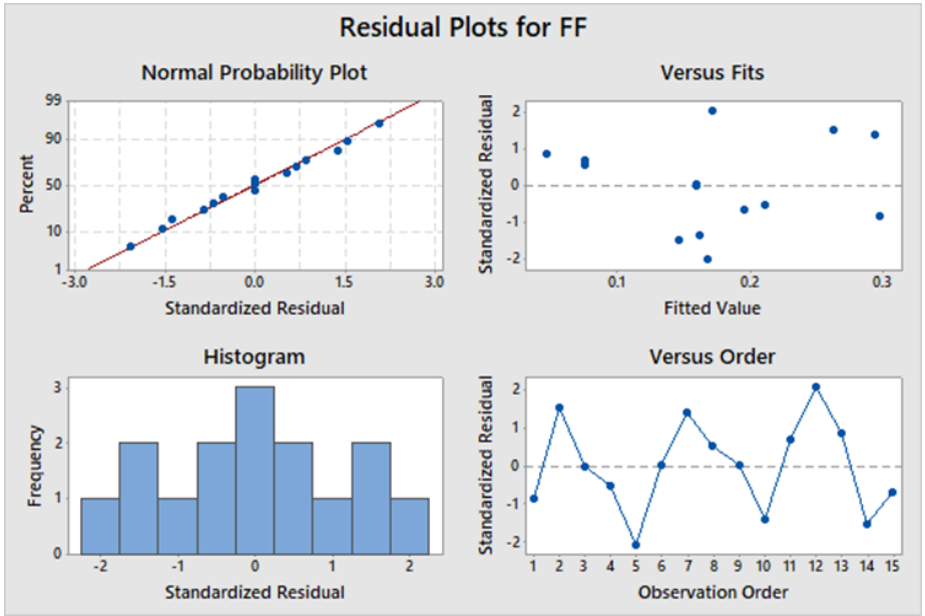

Fig. 8. Residual plot for friction factor

4. Conclusion

A CFD friction factor model of internal corrugated pipe flow has been verified and validated with the results obtained from the regression model. The response surface methodology has been used to determine three design factors' effects on the friction factor (response variable). The quadratic model obtained from the Box Behnken design (BBD) approach has been successfully developed. It reveals that three factors (i.e., Lw, a, Re) affect the friction factor in a significant manner.

Acknowledgement

The authors are grateful for the support from Universiti Tenaga Nasional (UNITEN), Agensi Nuklear Malaysia (ANM), Jabatan Perkhidmatan Awam Malaysia (JPA) and Rabdan Academy for their supports and helps in completing this work.

References

[1] Bigdeli, Masoud Bozorg, Matteo Fasano, Annalisa Cardellini, Eliodoro Chiavazzo, and Pietro Asinari. "A review on the heat and mass transfer phenomena in nanofluid coolants with special focus on automotive applications." *Renewable and Sustainable Energy Reviews* 60 (2016): 1615-1633. https://doi.org/10.1016/j.rser.2016.03.027

[2] Sidik, Nor Azwadi Che, M. M. Yassin, and M. N. Musa. "Turbulent-forced convective heat transfer and pressure drop analysis of Fe3O4 magnetic nanofluid in a circular microchannel." *Jurnal Teknologi* 75, no. 11 (2015). https://doi.org/10.11113/jt.v75.5293

[3] Wen, Dongsheng, Guiping Lin, Saeid Vafaei, and Kai Zhang. "Review of nanofluids for heat transfer applications." *Particuology* 7, no. 2 (2009): 141-150. https://doi.org/10.1016/j.partic.2009.01.007

[4] Ventola, Luigi, Francesco Robotti, Masoud Dialameh, Flaviana Calignano, Diego Manfredi, Eliodoro Chiavazzo, and Pietro Asinari. "Rough surfaces with enhanced heat transfer for electronics cooling by direct metal laser sintering." *International Journal of Heat and Mass Transfer* 75 (2014): 58-74. https://doi.org/10.1016/j.ijheatmasstransfer.2014.03.037

[5] Choi, S. US, and Jeffrey A. Eastman. *Enhancing thermal conductivity of fluids with nanoparticles*. No. ANL/MSD/CP-84938; CONF-951135-29. Argonne National Lab.(ANL), Argonne, IL (United States), 1995.

[6] Han, Huai-Zhi, Bing-Xi Li, Hao Wu, and Wei Shao. "Multi-objective shape optimization of double pipe heat exchanger with inner corrugated tube using RSM method." *International Journal of Thermal Sciences* 90 (2015): 173-186. https://doi.org/10.1016/j.ijthermalsci.2014.12.010

[7] Ny, G., N. Barom, S. Noraziman, and S. Yeow. "Numerical study on turbulent-forced convective heat transfer of Ag/Heg water nanofluid in pipe." *J. Adv. Res. Mater. Sci* 22, no. 1 (2016): 11-27.

[8] Permanasari, Avita Ayu, Muhammad Taufiq Affandi, Poppy Puspitasari, and Mirza Abdillah. "Optimization of manganese ferrite/distilled water parameter design on heat exchanger using RSM and CFD." In *IOP Conference Series: Materials Science and Engineering*, vol. 1034, no. 1, p. 012056. IOP Publishing, 2021. https://doi.org/10.1088/1757-899X/1034/1/012056

[9] Sajid, Muhammad Usman, and Hafiz Muhammad Ali. "Thermal conductivity of hybrid nanofluids: a critical review." *International Journal of Heat and Mass Transfer* 126 (2018): 211-234. https://doi.org/10.1016/j.ijheatmasstransfer.2018.05.021

[10] Bahiraei, Mehdi, Mohamad Berahmand, and Amin Shahsavar. "Irreversibility analysis for flow of a non-Newtonian hybrid nanofluid containing coated CNT/Fe3O4 nanoparticles in a minichannel heat exchanger." *Applied Thermal Engineering* 125 (2017): 1083-1093. https://doi.org/10.1016/j.applthermaleng.2017.07.100

[11] Bahiraei, Mehdi, Reza Rahmani, Ali Yaghoobi, Erfan Khodabandeh, Ramin Mashayekhi, and Mohammad Amani. "Recent research contributions concerning use of nanofluids in heat exchangers: a critical review." *Applied Thermal Engineering* 133 (2018): 137-159. https://doi.org/10.1016/j.applthermaleng.2018.01.041

[12] Gürbüz, Emine Yağız, Halil İbrahim Variyenli, Adnan Sözen, Ataollah Khanlari, and Mert Ökten. "Experimental and numerical analysis on using CuO-Al2O3/water hybrid nanofluid in a U-type tubular heat exchanger." *International Journal of Numerical Methods for Heat & Fluid Flow* 31, no. 1 (2021): 519-540. https://doi.org/10.1108/HFF-04-2020-0195

[13] Chein, Reiyu, and Jason Chuang. "Experimental microchannel heat sink performance studies using nanofluids." *International journal of thermal sciences* 46, no. 1 (2007): 57-66. https://doi.org/10.1016/j.ijthermalsci.2006.03.009

[14] Mukhtar, A., K. C. Ng, and M. Z. Yusoff. "Passive thermal performance prediction and multi-objective optimization of naturally-ventilated underground shelter in Malaysia." *Renewable Energy* 123 (2018): 342-352. https://doi.org/10.1016/j.renene.2018.02.022
[15] Yusoff, Mohd Zamri, Azfarizal Mukhtar, Khai Ching Ng, and Mohamad Fariz Mohamed Nasir. "Application of Box-Behnken design with response surface to optimize ventilation system in underground shelter." *Journal of Advanced Research in Fluid Mechanics and Thermal Sciences* 52, no. 2 (2018): 161-173.
[16] Kaood, A., T. Abou-Deif, H. Eltahan, M. A. Yehia, and E. E. Khalil. "Numerical investigation of heat transfer and friction characteristics for turbulent flow in various corrugated tubes." *Proceedings of the Institution of Mechanical Engineers, Part A: Journal of Power and Energy* 233, no. 4 (2019): 457-475. https://doi.org/10.1177/0957650918806407
[17] Ekiciler, Recep, Kamil Arslan, Oğuz Turgut, and Burak Kurşun. "Effect of hybrid nanofluid on heat transfer performance of parabolic trough solar collector receiver." *Journal of Thermal Analysis and Calorimetry* 143 (2021): 1637-1654. https://doi.org/10.1007/s10973-020-09717-5
[18] Tan, C., S. Zainal, C. J. Sian, and T. J. Siang. "ANSYS simulation for Ag/HEG hybrid nanofluid in turbulent circular pipe." *Journal of Advanced Research in Applied Mechanics* 23, no. 1 (2016): 20-35.
[19] Bellos, Evangelos, and Christos Tzivanidis. "Thermal analysis of parabolic trough collector operating with mono and hybrid nanofluids." *Sustainable Energy Technologies and Assessments* 26 (2018): 105-115. https://doi.org/10.1016/j.seta.2017.10.005
[20] Minea, Alina Adriana. "Hybrid nanofluids based on Al2O3, TiO2 and SiO2: numerical evaluation of different approaches." *International Journal of Heat and Mass Transfer* 104 (2017): 852-860. https://doi.org/10.1016/j.ijheatmasstransfer.2016.09.012
[21] Sundar, L. Syam, Korada Viswanatha Sharma, Manoj K. Singh, and A. C. M. Sousa. "Hybrid nanofluids preparation, thermal properties, heat transfer and friction factor–a review." *Renewable and Sustainable Energy Reviews* 68 (2017): 185-198. https://doi.org/10.1016/j.rser.2016.09.108
[22] Amani, Mohammad, Pouria Amani, Alibakhsh Kasaeian, Omid Mahian, and Somchai Wongwises. "Thermal conductivity measurement of spinel-type ferrite MnFe2O4 nanofluids in the presence of a uniform magnetic field." *Journal of Molecular Liquids* 230 (2017): 121-128. https://doi.org/10.1016/j.molliq.2016.12.013
[23] Esfe, Mohammad Hemmat, Hadi Hajmohammad, Davood Toghraie, Hadi Rostamian, Omid Mahian, and Somchai Wongwises. "Multi-objective optimization of nanofluid flow in double tube heat exchangers for applications in energy systems." *Energy* 137 (2017): 160-171. https://doi.org/10.1016/j.energy.2017.06.104
[24] Montgomery, Douglas C., George C. Runger, and Norma F. Hubele. *Engineering statistics*. John Wiley & Sons, 2009.
[25] Zarina Mohd Khalid, Norazlina Ismail, Norhaiza Ahmad, Noraslinda Mohamed Ismail, Arifah Bahar, Ismail Mohamad, Muhammad Hisyam Lee, and Muhammad Fauzi Hamdan, *Statistics For Engineers*. 2019, Johor, Malaysia: UTM PRESS. 187.
[26] Chiang, Ko-Ta, and Fu-Ping Chang. "Application of response surface methodology in the parametric optimization of a pin-fin type heat sink." *International communications in heat and mass transfer* 33, no. 7 (2006): 836-845. https://doi.org/10.1016/j.icheatmasstransfer.2006.04.011